Supporting Information

Ligand-Mediated Formation of Amphiphilic Silver Nanoclusters: Synthesis, Redox Properties, and Activity against Clinically Relevant Bacteria

Alexandru-Milentie Hada,[a] Marco Abbate,[b] Markus Zetes,[a] Ana Laura Coria-Gutiérrez,[b] Ana-Maria Craciun,[a] Nina Burduja,[b,c] Chiara Abate,[b] Francisco J. Terán,[d] Milica Todea,[a,f] Antonino Mazzaglia,[c] Angela Scala,[b] Antonia Nostro,[b] and Anna Piperno[b*]

[a]. Interdisciplinary Research Institute in Bio-Nano-Sciences, Babes-Bolyai University, T. Laurian Str. 42, 400271 Cluj-Napoca, Romania.

b. Department of Chemical, Biological, Pharmaceutical and Environmental Sciences, University of Messina, V.le F. Stagno d'Alcontres 31, 98166 Messina, Italy. E-mail: apiperno@unime.

c. National Research Council, Institute for Nanostructured Materials (CNR-ISMN), URT of Messina at Dept. of Chemical, Biological, Pharmaceutical and Environmental Sciences (ChiBioFarAm), University of Messina, Viale F. Stagno d'Alcontres 31, 98166 Messina, Italy

d. Nanotech Solutions, Ctra Madrid 23, 40150 Villacastín, Spain

e. Faculty of Nursing and Health Sciences, Iuliu Haţieganu University of Medicine and Pharmacy, Victor Babeş 8, RO-400012 Cluj-Napoca, Romania

*Corresponding author at: Department of Chemical, Biological, Pharmaceutical and Environmental Sciences, University of Messina, V.le F. Stagno d'Alcontres 31, 98166 Messina, Italy. E-mail: apiperno@unime.it.

TABLE OF CONTENT

Physicochemical Characterization

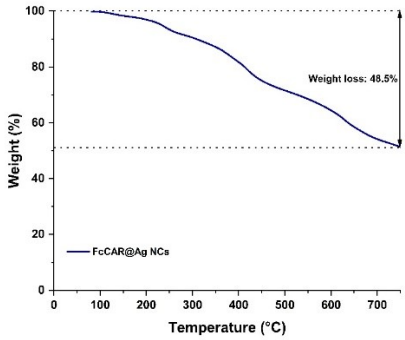

Fig. S1. TGA of FcCAR@Ag NCs.

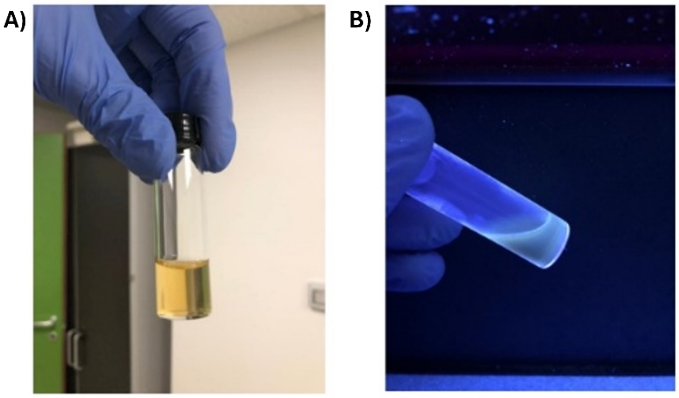

Fig. S2. (A) Brownish FcCAR@Ag NCs solution under ambient light; (B) FcCAR@Ag NCs solution under UV irradiation:

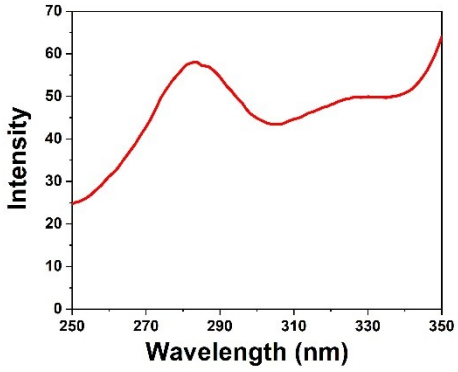

a bluish emission is observed.

Fig. S3. Fluorescence excitation spectra of FcCAR@Ag NCs (λ_{em}= 425 nm).

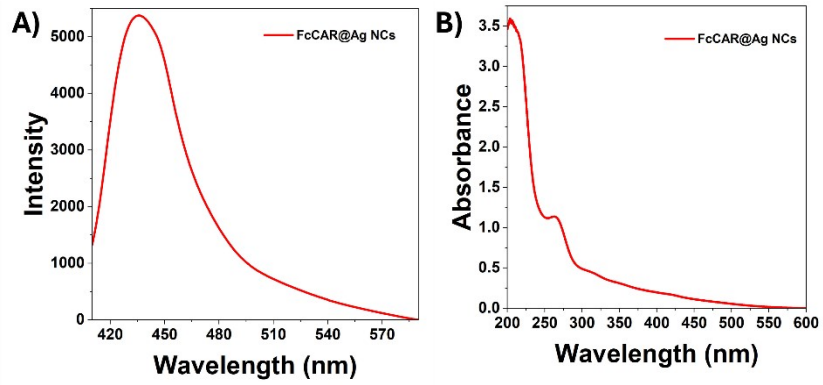

Fig. S4. UV-Vis and fluorescence emission spectra of stored FcCAR@Ag NCs samples ([FcCAR]= 220 µM, path length = 1 cm, λ_{exc}= 390 nm).

High-Resolution XPS Analysis

XPS analysis was carried out to determine the elemental composition of FcCAR and FcCAR@Ag NCs and gain deeper insight into the interaction between Ag NCs and FcCAR molecules. The elemental composition at the surface of the samples (up to 10 nm the depth of XPS analysis) derived from the survey spectra is summarized in Table S1. Comparison of the surface atomic concentrations reveals a decrease in carbon and nitrogen, alongside an increase in oxygen, sodium, and iron content in the FcCAR@Ag NCs respect to FcCAR sample. The very low atomic concentration of Ag, around 0.1% for FcCAR@AgNCs suggests that the FcCAR effectively covers the Ag nanoclusters. Furthermore, in FcCAR@AgNCs the O/C ratio increases, and the deconvolution of high-resolution C 1s spectrum shows a slightly increased total contribution of O–C=O and C=O components. These findings suggest that FcCAR molecules surrounding the AgNCs are oriented with the ends containing Fe (in ferrocenyl) and O=C-N, O=C-Na groups outwards and with the imidazole (C and N-containing) ring in towards the core Ag NCs. The high-resolution C 1s spectra recorded for the two samples have an asymmetric shape. The width of the peaks allowed a deconvolution using four components (Fig. S6A). The results are summarized in Table S2. At lower binding energies, of around 284.6 eV, there is a component attributed to the carbon atom involved in C–C/C–H bonds. This component was used as a reference for the calibration of all recorded XPS spectra. The second component at around 285.5 eV can be due to the C–N bonds in FcCAR molecules and/or C–O coming from the contaminating carbon due to the atmospheric exposure of the samples[1]. The component at 287.7 eV is attributed to the carbon in the C=O and/or imidazole's N=C– NH bonds[2]. The last peak of carbon assigned to carboxylate (O=C–OH) and amide (N–C=O) carbon appeared at a binding energy higher than 289eV [3]. The decrease in the intensity of the signals associated with the imidazole rings, namely N=C–NH bonds, together with the increased intensity of the peak corresponding to O=C–OH and amide N–C=O bonds, suggests that the FcCAR molecules are oriented around the Ag NCs with the imidazole ring directed toward the interior. The deconvolution of the XPS O 1s spectra for both samples (Fig. S6D, Table S3) was carried out using two main components. The peaks position corresponds to C=O/ O-C=O groups at approximately 531eV and C-O, [OH]-related species around 534eV[4], the latter originating from organic surface contamination and water adsorbed on the sample surfaces[4]. For

FcCAR@Ag NCs sample, an additional component at a higher binding energy, around 536 eV, was included in the fitting procedure and attributed to the sodium Auger peak (Na KLL), further confirming the elemental composition of the sample. As illustrated in Fig. S6D, no peaks associated with AgO or Ag2O species are observed in the lower binding energy region of the O 1s spectra around 528–529 eV. This finding indicates that silver remains unoxidized during the synthesis of the FcCAR@Ag NCs[4]. The high-resolution N 1s spectra and their deconvolutions for the FcCAR and FcCAR–Ag NCs samples are shown in Fig. S6C, while the fitting results are summarized in Table S4. Both spectra were well fitted using two spectral components centred at 399 and 400.2 eV, respectively. The lower binding energy component was assigned to imino nitrogen (C–N=C, imine ring), whereas the higher binding energy component was attributed to C–NH–C bonds. The relative contributions of the two components remained nearly unchanged for both samples, indicating that the presence of Ag did not lead to the formation of new nitrogen-related chemical bonds. The full width at half maximum of the N1s peak for the Ag-containing sample narrows from 2.88 eV to 2.44 eV, which indicates a more ordered arrangement of FcCAR molecules around the Ag NCs. The Fe 2p spectra provide important evidence for the presence of the ferrocene moiety in the FcCAR molecule. For both samples, the peak positions remain essentially unchanged, indicating the absence of significant shifts in binding energy, although an increase in peak intensity is observed for the FcCAR@Ag NCs sample (Fig.S6B and Table S5). The detected peaks for both samples are characteristic of iron in the low-spin Fe(II) state within the cyclopentadienyl rings, with the Fe 2p3/2 and Fe 2p1/2 signals located at approximately 708.0 and 720.5 eV, respectively.

The peaks recorded in the Ag 3d photoelectron region for both samples are shown in Fig. 7. XPS spectra shows for FcCAR@Ag NCs sample the presence of characteristic Ag 3d5/2 and Ag 3d3/2 peaks at binding energies of 368.6 and 374.7 eV which are in good agreement with binding energies for Ag NPs values[4]. The valence band region provides a distinctive fingerprint of electronic hybridization between Ag and C. The valence band structure of silver is mainly characterized by populated 4d orbitals, which form a narrow band located between 4-8 eV below the Fermi level[5]. The formation of Ag–C bond is associated with hybridization between Ag 4d and C 2p orbitals, leading to spectral modifications[4]. A detailed comparison of the valence band spectra for both samples highlights the contributions from Fe 3d, C 2s, C 2p, and O 2p orbitals. For the AgNCs@FcCAR sample, a distinct and intense peak appears at a binding energy of approximately 2.2 eV, attributed to Ag 4d states[5], while this feature is absent in the FcCAR sample. Specifically, a shift of Ag4d peak toward lower binding energies is observed. In addition, the C 2s peak located at approximately 11.7 eV becomes more pronounced in the Ag-containing sample, indicating possible hybridization between the Ag 4d and C 2p orbitals[4]. Notably, the energy separation between Ag4d and C2s matches the intrinsic energy difference between C 2p and C 2s orbitals (~8.5 eV) in free carbon atoms, further supporting the hypothesis of Ag–C bond formation between the AgNC core and the FcCAR shell.

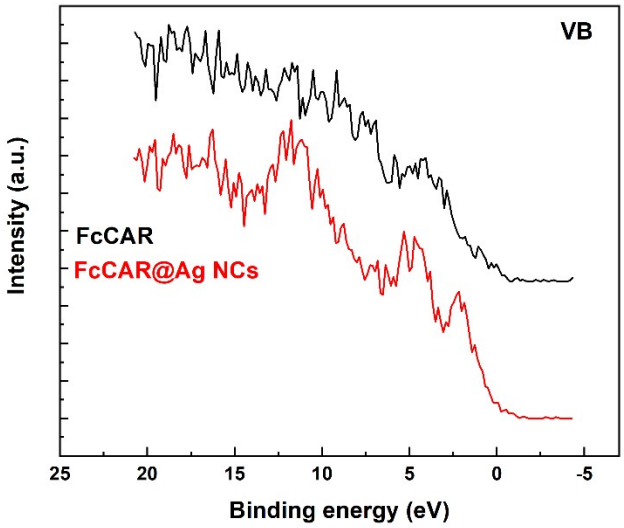

Fig. S5 XPS Valence band spectra of FcCAR and FcCAR@ Ag NCs.

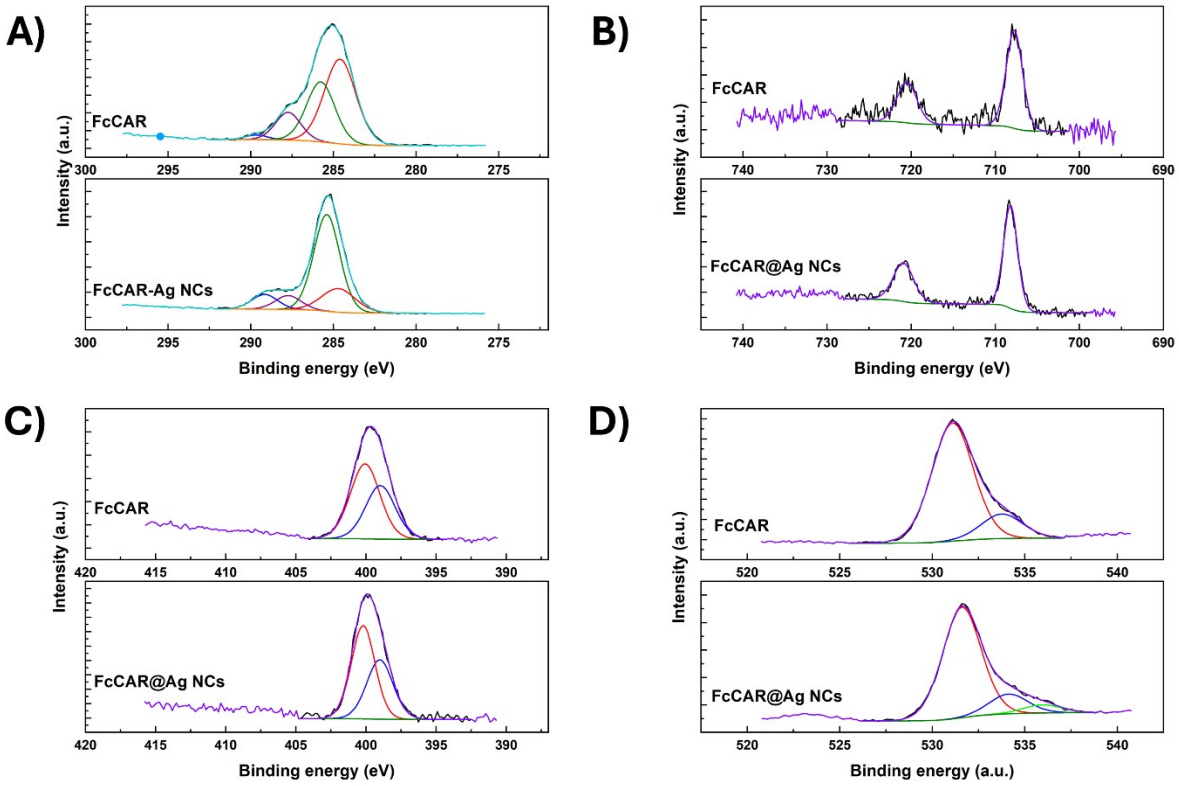

Fig. S6 XPS spectra of (A) C1s,(B) Fe2p, (C) Nis, and (D) O1s.

Table S1. Elemental composition (at%) on the surface of the samples was determined from the survey spectra

Sample	At% of the elements					
	O	C	N	Na	Fe	Ag
FcCAR	18.3	68.6	11.6	0.9	0.6	-
FcCAR@Ag NCs	21.3	66.8	6.5	4.1	1.2	0.1

Table S2. Results from the deconvolution of C1s spectra

Sample	C-C /C-H	%	C-N /C-O	%	C=O N=C–NH (IM-ring)	%	O=C–OH, N–C=O	%
FcCAR	284.6	51.5	285.7	32.9	287.7	13.6	289.7	2
FcCAR@Ag NCs	284.6	19.6	285.4	61.9	287.7	8.9	289.1	9.4

Table S3: Results from the deconvolution of O1s spectra

Sample	C=O O-C=O	%	OH (H2O) C-O surface contamination	%	Na KLL Auger	%
FcCAR	531.1	82.8	533.8	17.2	-	-
FcCAR@Ag NCs	531.6	79.9	534	14.3	535.9	5.8

Table S4: Results from the deconvolution of N1s spectra

Sample	C-N=C	%	C-NH-C	%
FcCAR	399	41.7	400.1	58.3
FcCAR@Ag NCs	399	41.4	400.2	58.6

Table S5: Results from the deconvolution of Fe2p spectra

Sample	Fe2p3/2	%	Fe2p1/2	%
FcCAR	707.7	66.6	720.5	33.4
FcCAR@Ag NCs	708.1	64.6	720.8	35.4

Table S6. Ag3d

Sample	Ag3d5/2	%	Ag3d3/2	%
FcCAR	-	-	-	-
FcCAR@Ag NCs	368.6	60	374.7	40

References:

1 M. Zetes, A. Hada, M. Todea, L. I. Gaina, S. Astilean and A. Craciun, *Nanoscale Adv.*, 2023, **5**, 5810–5818.
2 Z. Xu, S. Yuan, H. Yan and C. Liu, *Colloids Surfaces A Physicochem. Eng. Asp.*, 2011, **380**, 135–142.
3 S. K. Das, C. Dickinson, F. Brougham and E. Marsili, *Green Chem.*, 2012, **14**, 1322.
4 D. W. Boukhvalov, I. S. Zhidkov, E. Z. Kurmaev, E. Fazio, S. O. Cholakh and L. D. Urso, *Carbon N. Y.*, 2018, **128**, 296–301.
5 L. Bech, Z. Li and J. Onsgaard, *J. Electron Spectrosc.*, 2007, **158**, 102–106.

Electrochemical Investigation

The electroactive surface area A (in cm2) is calculated according to the Randles–Ševčik equation:

$$i_{a,p} = (2.69 \times 10^5)\, n^{3/2}\, A\, c\, v^{1/2} D^{1/2}$$

where 2.69 x 105 is a constant (C V1/2/mol), n is the number of electrons transferred (in mol), c is the concentration of solution (mol/cm3) and D is the diffusion coefficient (cm2/s), calculated by Nicholson method along with the electron transfer constant k0 (D = 5.71 x 10-6 cm2/s, k0> v1/2)[6–8]. The values of A result in 0.016 cm^2 and 0.044 cm^2 for FcCAR and FcCAR@AgNCs, respectively. The increase in A value for FcCAR@AgNCs (A of FcCAR@AgNCs ~2.7 > A of FcCAR) is consistent with the presence of nanoclusters on the electrode surface, which increases the surface-to-volume ratio and introduce a large number of active sites. This factor, along with the assembly of FcCAR on the NCs surface, may underlie the enhanced electron transfer efficiency and highlight the potential of FcCAR@Ag NCs in electroanalytical applications, thereby corroborating what has been reported in the literature [9].

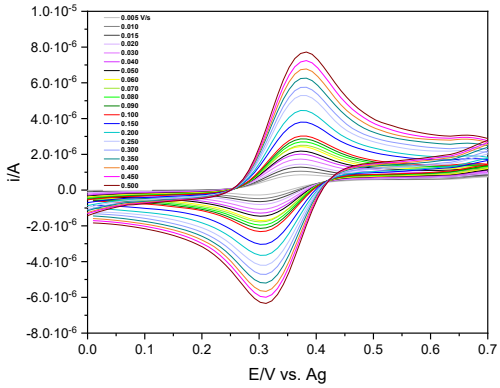

Fig. S7 Scans in CV of FcCAR (1 mM) in KCl (0.1M) on SPCE under different scan rate values (0.005 ≤ v/ V/s ≤ 0.500).

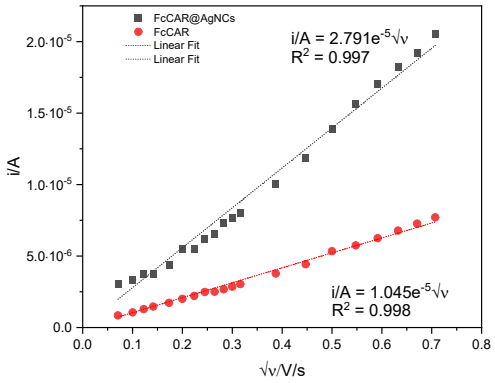

Fig. S8. Calibration plot of $i_{a,p}$ **values (from CV scans) vs. √*v* or Randles-Sevcik plot.**

References:

6 M. G. Trachioti, A. Ch and L. Mamas, *Microchim. Acta*, 2023, 1–14.

7 N. Aristov and A. Habekost, *World J. Chem. Educ.*, 2015, **3**, 115–119.

8 H. Yamada, K. Yoshii, M. Asahi, M. Chiku and Y. Kitazumi, *Electrochemistry*, 2022, **90**, 1–8.

9 M. Chirea, C. M. Pereira and F. Silva, *J. Phys. Chem. C*, 2007, **11**, 9255–9266.

Antibacterial activity

Table S7. MIC values of clinically relevant antibiotics: vancomycin was used as positive control for Gram-positive bacteria and ciprofloxacin as positive control for both Gram-positive and Gram-negative strains.

Bacteria	Ciprofloxacin (μg/mL)	Vancomycin (μg/mL)
S. aureus ATCC 6538	0.125	1
E. coli ATCC 10536	0.125	>512
S. aureus (MRSA) ATCC 43300	0.25	1
E. faecium (VREfm) DSM 17050	0.5	512
E. coli DSM 105388	8	>512
P. aeruginosa ATCC 9027	0.125	>512

Biocompatibility of FcCAR@Ag NCs

Cell culture Human skin fibroblasts WS1 were purchased from American Type Culture Collection (ATCC® CRL-1502™) and cultured in MEM α (Minimum Essential Medium α, nucleosides, no ascorbic acid; Gibco A10490-01) supplemented with 10% Fetal Bovine Serum (FBS; Gibco A5256701) and 1% penicillin/streptomycin (P/S; Gibco 15140-122), hereafter referred to as cell media. Once the confluence was reached, cells were detached from the flask by trypsinization and centrifuged. The cell number and viability were assessed by Trypan Blue Dye Exclusion Test. Cells were then seeded in cell media in 96-well plates at a density of 5000 cells/well. The day after, the media was removed, and cell media containing the FcCAR@Ag NCs at 23.37 μg/mL and 11.68 μg/mL, was added for 24 hours to assess cytotoxicity. All cell-handling procedures were performed under a sterile laminar flow hood, and cell cultures were incubated at 37°C with 5% CO_2 under controlled humidity conditions.

Cytotoxicity tests: A quantitative analysis of the compounds' cytotoxicity was performed using PrestoBlue Cell Viability Reagent (Invitrogen) following the manufacturer's instructions. Briefly, 24 hours after FcCAR@Ag NCs administration, cells were incubated with 10% (v/v) PrestoBlue Reagent for 2 h at 37 °C, 5% CO2. The samples were analysed in triplicate using a Fluoroskan Microplate Fluorometer (Thermo Fisher Scientific) at 544 nm excitation and 590 nm emission. The data were represented as a percentage of viable cells with respect to the not treated cells, used as a control.

Statistical analysis All results are presented as mean ± Standard Error of the Mean (SEM). Statistical analyses were performed by Two-Way ANOVA and, Tukey's, multiple comparisons test, using OriginPro (OriginLab, 2026). Statistical significance is indicated on graphs as: *p ≤ 0.05, **p ≤ 0.01, ***p ≤ 0.001, and ****p ≤ 0.0001.

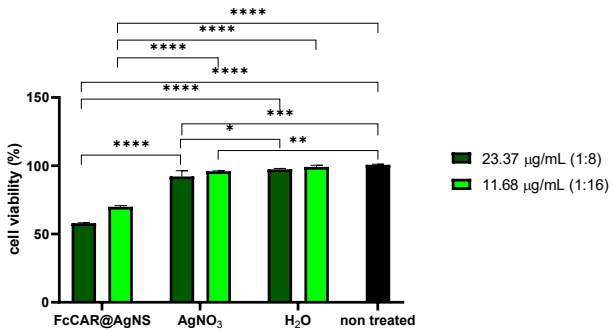

Fig. S9. Cell viability analysis. Cell viability was assessed using the PrestoBlue assay after 24 h of culture with NCs at concentrations of 23.37 μg/mL and 11.68 μg/mL. Data are presented as mean ± standard error (SE) of the percentage of viable cells relative to untreated control cells. Statistical significance is indicated as follows: *p ≤ 0.05; **p ≤ 0.01; ***p ≤ 0.001; ****p ≤ 0.0001.